Malaysian Journal of Analytical Sciences, Vol 23 No 3 (2019): 423 - 435
DOI: https://doi.org/10.17576/mjas-2019-2303-06

MALAYSIAN JOURNAL OF ANALYTICAL SCIENCES
Published by The Malaysian Analytical Sciences Society
ISSN 1394 - 2506

VALIDATION ON CARBON DIOXIDE HYDRATE FORMATION THROUGH ANALYSIS ON THE SOLUBILITY OF CO_2 IN WATER USING HENRY'S LAW AND THE EXPERIMENTAL PRESSURE-TIME CURVE

(Mengesahkan Pembentukan Hidrat Karbon Dioksida Melalui Kajian Terhadap Kadar Keterlarutan CO_2 di dalam Air Menggunakan Hukum Henry dan Graf Tekanan-Masa)

Mohd Hafiz Abu Hassan[1]*, Colin Edwards Snape[2], Lee Stevens[2]

[1]*Faculty of Science and Technology,*
Islamic Science University of Malaysia, Bandar Baru Nilai, 71800 Nilai, Negeri Sembilan, Malaysia
[2]*Cleaner Fossil Energy and Carbon Capture Technologies Research Group, Faculty of Engineering,*
University of Nottingham, NG7 2TU Nottingham, United Kingdom

**Corresponding author: mhafiz.a.h@usim.edu.my*

Received: 21 September 2017; Accepted: 3 May 2019

Abstract

A rise of 2 ^oC in the Earth's temperature is likely to occur when the concentration of carbon dioxide (CO_2) in the atmosphere reaches approximately 450 ppm. CO_2 emissions are closely related to the continual use of fossil fuels. In order to make fossil fuels sustainable, carbon capture and storage (CCS) is required to reduce CO_2 emissions. CO_2 hydrate (CO_2:$6H_2O$) formation has been investigated as a way to capture CO_2. The formation of hydrate in this work was experimentally investigated in batch mode inside a vertical fixed-bed reactor (FBR), also known as high-pressure volumetric analyser (HPVA). Standard silica gel with an average particle size of 200–500 µm, mean pore size of 5.14 nm, a pore volume of 0.64 cm^3/g, and a surface area of 499 m^2/g was used as a porous medium. The presence of hydrate in FBR was justified by using graphic methods. The solubility of CO_2 in water using Henry's law and the experimental pressure–time (P-t) curve were analysed to determine the formation of hydrate. Hydrate formation was confirmed when the mole fraction of CO_2 dissolved in water exceeded the Henry's law value as well as a two-stage pressure drop in the experimental P-t curve.

Keywords: greenhouse effect, carbon dioxide hydrate, silica gel, Henry's law, pressure-time curve

Abstrak

Kenaikan suhu bumi sebanyak 2 ^oC berkemungkinan terjadi apabila kandungan karbon dioksida di persekitaran mencapai lebih kurang 450 ppm. Pembebasan CO_2 berkait rapat dengan penggunaan bahan api fosil yang berterusan. Bagi menghasilkan bahan api fosil yang mampan, simpanan dan perangkap karbon (CCS) diperlukan untuk mengurangi pelepasan CO_2. Formasi CO_2 hidrat telah dikaji untuk memerangkap CO_2. Pembentukan hidrat telah dikaji untuk memerangkap karbon dioksida melalui eksperimen yang dijalankan menggunakan reaktor (FBR), juga dikenali sebagai penganalisa volumetrik tekanan tinggi (HPVA). Gel silika dengan purata saiz 200–500 µm, purata diameter liang 5.14 nm, isipadu liang 0.64 cm^3/g, dan luas permukaan 499 m^2/g telah digunakan sebagai medium untuk pembentukan hidrat. Pembentukan hidrat di dalam reaktor disahkan melalui kaedah analisis graf. Kadar keterlarutan CO_2 di dalam air dan graf tekanan-masa dikaji untuk menentukan pembentukan hidrat. Pembentukan hidrat disahkan apabila bilangan mol CO_2 yang larut di dalam air melebihi nilai hukum Henry dan juga dua peringkat penurunan tekanan dapat dilihat dalam lengkung experimen P-t.

Kata kunci: kesan rumah hijau, hidrat karbon dioksida, gel silica, hukum Henry, graf tekanan-masa

Introduction

Human activities since the Industrial Revolution, such as burning coal, natural gas, and oil, to power machines for manufacturing and transportation have now increased the concentration of CO_2 (type of greenhouse gases) in the atmosphere, intensifying the natural warming caused by the greenhouse effect [1]. Biello reported that CO_2 levels in the atmosphere have reached 400 ppm for the first time in at least 800,000 years [2], which is far above the value recorded before the Industrial Revolution: 280 ppm [1]. Biello also stated that global temperatures are estimated to rise by 2 ^{o}C if the concentration of CO_2 in the atmosphere reaches 450 ppm [2].

With the persistent use of fossil fuels, the capture of CO_2 needs to be considered [3] where International Energy Agency (IEA) highlighted that carbon capture and storage (CCS) has been a favorable mitigation against climate change by 2050 [4]. There are three leading technologies for CO_2 capture, namely post-combustion capture, pre-combustion capture at IGCC plants, and oxy-fuel combustion. Post-combustion capture can be attained in the flue gas stream emitted from conventional steam power plants, entailing the separation of CO_2 from the flue gas mixture. Oxy-fuel combustion is a process where a fuel is combusted with oxygen (O_2) in a nitrogen (N_2)-free environment to produce a flue/exhaust gas consisting of CO_2 and water (H_2O). While the main concept of pre-combustion is to produce fuel gas containing mostly CO_2 and H_2 (an attractive future clean energy source) emitted in the range between 283–290 K at a pressure range of 20–70 bar [5].

D'Alessandro et al. [6] highlighted several promising new materials for CO_2 capture methods such as physical or chemical absorbents, adsorption of solids, cryogenic systems, membranes, hydrate-based gas separation (HBGS), and chemical looping combustion by metal oxides. HBGS is one of the most promising approaches in CO_2 capture field [7–10]. This CO_2 capture method involves clathrate or gas hydrate crystallization and can be applied to both post- (from flue gas) and pre-combustion (from fuel gas) capture, respectively. However, the HBGS process is more suitable for pre-combustion CO_2 capture from a fuel gas mixture than a flue gas mixture because the partial pressure of the shifted fuel gas (40% CO_2 and 60% H_2) is up to 1,000 times higher than that of the flue gas (17% CO_2 and 83% N_2) in post-combustion capture [11]. Thus, HBGS has been chosen in this study because the CO_2 hydrate formation is a continuous operation, thus making it possible to treat a large amount of gaseous stream, recovering more than 99 mol% of CO_2 from the fuel gas [12].

The HBGS process relies on the ability of water to form non-stoichiometric crystalline compounds in the presence of CO_2, N_2, O_2, and H_2, as well as natural gas components at high pressures (10–70 bar) and low temperatures (near 273 K) [6]. Mainly, there are three conditions necessary for hydrate formation to occur: (i) low temperature and high pressure are needed for these solid compounds to form from pure water, depending on the physical and chemical properties of the guest molecule; (ii) guest molecules must be present such as methane, ethane, or carbon dioxide; (iii) a sufficient amount of water, not too much and not too little [13]. Carrol [13] also stated that the CO_2 hydrate formation conditions are in the range of 273.15–283 K at the pressure range of 12.7–45 bar, wherein this is the case for a pure CO_2 system. A number of techniques have been investigated by researchers to capture CO_2 with gas hydrate formation by implementing the most traditional way (bulk water), solid adsorbent (porous medium), and promoters (oxygenated solvents, surfactants, semi-clathrate hydrate, and hydrophobic former). However, the focus of this study was to justify the formation of hydrate inside fixed-bed reactor (FBR) or HPVA, wherein silica gel was used as a solid adsorbent (porous medium) to omit the need of stirring process inside the reactor.

Most of the experiments that used silica saturated with water inside FBR have shown greater CO_2 uptake as compared to bulk water in a stirred tank reactor (STR). Adeyemo et al. [14] investigated clathrate crystallization in a silica gel column from fuel gas mixture at the operating conditions of 272.15 K and 70 bars, respectively. Three different silica gels were used (gel 1 with a pore size of 30 nm and particle size of 40–75 μm; gel 2 with a pore size of 100 nm and particle size of 40–75 μm; gel 3 with a pore size of 100 nm and particle size of 75–200 μm) and the highest CO_2 composition in hydrate was observed for gel 3 around 92 mol% (CO_2 uptake of 2 mmol of CO_2 per g of H_2O). Kumar et al. [15] employed three types of silica gel (mesh size of 60–120 (type A), 100–200 (type B), and 230–400 (type C)), which had almost similar pore diameters and different surface areas with type C having the highest surface area and type A the lowest. The CO_2 uptake obtained at 274 K and 36 bars in pure CO_2 indicated silica gel with larger surface area (type C) led to the higher gas consumption as well as reduced the induction time.

The conversion of water to hydrate for type C was 50 mol%, which was 20% higher than type B and almost 50% higher than type A.

Park et al. [16] studied the hydrate phase equilibria for the fuel gas and water mixtures inside various sizes of silica gel pores and concluded that silica gel with the highest pore diameter exhibited the best driving force for hydrate formation that was close to the bulk water. They mentioned that the capillary effect due to the presence of geometrical constraints caused the equilibrium lines to be shifted to the inhibition region, which was to the left side of the bulk water system. They added that this effect was more significant at smaller pore sizes (6.0 nm) due to the decreased activity of water caused by the partial ordering and bonding of water molecules with hydrophilic surfaces of pores. Kang et al. [17] conducted an investigation on three different silica gel pores (25 nm, 100 nm, and 250 nm) at the operating conditions of 274.15 K and 60 bar, and the observed phase equilibria justified the statement made by Park et al. [16] in which silica gel with pore size of 25 nm demonstrated the highest inhibition effect.

Babu et al. [12] employed silica sand (average pore diameter of 329 µm and pore volume of 0.22 cm^3/g) and silica gel (average pore diameter of 100 nm and pore volume of 0.83 cm^3/g) as the solid beds in the reactor to explore the formation of hydrate from fuel gas mixture at the operating temperature of 274.15 K and three different pressures (75 bar, 85 bar, 90 bar). Silica sand demonstrated better CO_2 capture capability with a 36 mol% conversion of water to hydrate which was almost two-thirds higher than silica gel. Further work on silica sand was performed by Mekala et al. [18] at different particle sizes (0.16 mm, 0.46 mm, and 0.92 mm), wherein 0.46 mm silica sand was found to have the optimum CO_2 uptake and rate of hydrate formation. Other than silicas, there are two more solid adsorbents being investigated by the researchers in the HBGS field, which are zeolites [18–21] and glass beads [22]. Xiaoya et al. [19] proved that the formation of CH_4 hydrate inside zeolite A-type pores is possible. Zhong et al. [20] conducted an investigation using zeolite 13X in FBR for the HBGS process from a CO_2/CH_4 gas mixture (40 mol% CO_2 and 60 mol% CH_4) at 277.15 K and in the pressure range of between 52–67 bar. They found that hydrate growth in the fixed-bed zeolite 13X was improved as the driving force increased from 25 bar to 40 bar. However, the comparison with STRs showed that the selectivity towards hydrate formation was lower for the fixed bed of zeolite 13X due to the massive moisture content available inside the pores, which increased the geometrical constraint or capillary effect [17]. Hence, they concluded that zeolite 13X can be used to enhance hydrate formation, but may not be a proper candidate for CO_2 capture from the CO_2/CH_4 gas mixture.

Recently, a number of parameters have been investigated to improve the gas uptake of hydrate formation inside the FBR, such as altering porous medium parameters used inside the reactor, varying the concentration of promoters, and employing different types of reactor orientations. Also, a majority of the researchers has used batch mode [23] to investigate hydrate formation in fuel gas mixture as an alternative to semi-batch mode. Additionally, Babu et al. [24] said that for the commercialization of HBGS, the use of FBR in batch mode was proposed by Babu et al. [25] which is similar to an industrial process namely Skarstrom cycle [26]. Also, they said this HBGS cycle can be conducted in a four step batch process namely, pressurization, hydrate formation, depressurization or thermal stimulation (H_2 rich), and hydrate decomposition (CO_2 rich). Moreover, Babu et al. [25] said the proposed cycle involves two fixed-bed columns and enables a continuous operation similar to how a pressure swing adsorption cycle would operate [27].

Additionally, Babu et al. [8] managed to observe hydrate formation by employing 5.53 mol% THF and 0.3 mol% TBAB in batch mode (1.5 cm bed height of silica sand), respectively, at 279 K and 60 bars. Then, Zheng et al. [7] managed to obtain CO_2 uptake of 2.4 mmol of CO_2 per g of H_2O at 283 K and 60 bars by employing 5.56 mol% THF inside a horizontal batch FBR (100 nm silica sand was used as porous media). They also discovered that this horizontal orientation had 1.5 times higher gas uptake as compared to the common (vertical) orientation. This new finding demonstrates the continuous interest by researchers to ensure that CO_2 hydrate can be used as a promising method for CCS by exploiting the advantages of porous medium in FBR such as those examined in this work by employing the HPVA. However, because of its limitation in which the formation of hydrate could not be seen directly by the eyes, there was no hydrate formation investigation being performed by using the HPVA previously. Thus, two approaches were used to justify the formation of hydrate in this work: analysis of P-t curves [28] and study of CO_2 dissolution in water suggested by Servio et al. [29].

Theoretically, the mechanism of hydrate formation can be described through a P-t curve, as explained by Tang et al. [28] with three phases: dissolution, nucleation, and hydrate growth. The decrease in the initial pressure of the system indicates the dissolution phase of hydrate formation, wherein labile cluster will form immediately. Later, the pressure becomes constant, indicating the nucleation phase of hydrate formation where labile clusters will agglomerate to form dodecahedral, tetrakaidecahedral, or hexakaidecahedral clusters. Finally, when the size reaches a critical value, growth begins. The hydrate growth phase is represented by subsequent curve/s that can be observed after the nucleation phase on the P-t curve. Thus, this will be a basic guideline to determine the formation of CO_2 hydrate in this work together with the study on CO_2 dissolution in water, wherein Servio et al. [29] plotted the equilibrium mole fraction of CO_2 in water in the presence of hydrate at various operating temperatures and pressures. This study will help validate the formation of hydrate inside any reactor where visuality is the main issue, as experienced in this work through the HPVA.

Materials and Methods

Materials and apparatus

Standard silica gel [21, 23, 31] was purchased from Fisher Scientific. CO_2 gas with a purity of 99.99% (maximum 103 bar), He gas with purity of 99.99% (34.4 bar) for venting or cleaning purposes, and N_2 gas/compressed air (5.2–5.5 bar) to control the pneumatic valves of the HPVA were supplied by BOC (a member of the Linde Group). All the materials were used without further purification.

The high-pressure volumetric analyser (model HPVA-100) that consists of constant temperature bath or water bath, vacuum pump, and degassing unit was manufactured by Micromeritics. The oven used (Model AX30) was manufactured by Carbolite and has a maximum temperature of 250 ^oC and a minimum temperature of 40 ^oC. The weighing balance (Model: AEA – 220A) used was manufactured by AE Adam and it can measure a maximum mass up to 220 g and a minimum mass of 10 mg. The high-speed blender was used to vigorously mixed silica gel with water [21, 23, 31].

Sample preparation method

Silica gel was initially dried inside the oven for one night at 200 ^oC. Dry silica gel (0.5 g) was placed inside blender and water was added in excess (19 times the mass of dry silica gel) so that the total mass of the mixture was 50 g. The silica gel and water mixture were vigorously stirred at the speed of 37000 rpm [30, 31] for 90 seconds using a high-speed blender. Then, the mixture was left at atmospheric condition until the final mass reached equilibrium. Finally, the amount of equilibrium moisture content inside silica gel pores was measured by using a degassing unit. The amount of water content was necessary to calculate the final conversion of water to CO_2 hydrate.

CO_2 hydrate formation

The system was manually purged with He gas three times to clean the line from any impurities. Next, the operating conditions, such as experiment time (in minute), analysis gas port, operating pressure (in bar), and temperature (in K), were pre-defined. After that, the sample cell was charged with wet silica gel and was placed inside water bath. The mixture of 70 vol% water + 30 vol% antifreeze was used to avoid the formation of ice inside water bath and to make sure that the water mixture was consistently circulated throughout the process. The cell's valve was initially closed.

Before the commencement of each experiment, the cell was pressurized to required pressure through a supply vessel containing CO_2 gas with a purity of 99.99%, and at the same time the desired operating temperature was established through constant temperature bath. After the operating conditions were achieved, the cell's valve was fully opened. Subsequently, the experiment for hydrate formation was left running for 1,200 minutes.

After the completion of each experiment, the pressure was reduced to atmospheric pressure at the same operating temperature for hydrate decomposition. Then, the system was automatically vented with He gas several times to clean the line for the next experiment. Subsequently, the cell's valve was fully closed and the sample cell was removed from the HPVA. Finally, the pressure–time (P-t) curve obtained after completion of the experiment was analysed to calculate the conversion of water to hydrate, CO_2 uptake, and rate of hydrate formation [31].

Results and Discussion

The formation of hydrate in the HPVA was examined by studying the P-t curves obtained together with the study of CO_2 dissolution in water according to Henry's law [29, 32], and then followed by analysis of CO_2 uptake and rate of hydrate formation. Three sets of experiments were performed for each sample and some control experiments were performed to distinguish between hydrate formation and physical adsorption by using the HPVA. The study on various driving forces towards hydrate formation was also presented.

Validation on CO_2 hydrate formation: P-t curve

All prepared samples were used to investigate hydrate formation in the HPVA at 275 K and 35 bars by using pure CO_2 gas (99.99% purity). As seen in Figure 1, the two-stage pressure drop trend was observed during the hydrate formation experiment where the total pressure drops achieved after 1,200 minutes was around 2 bar.

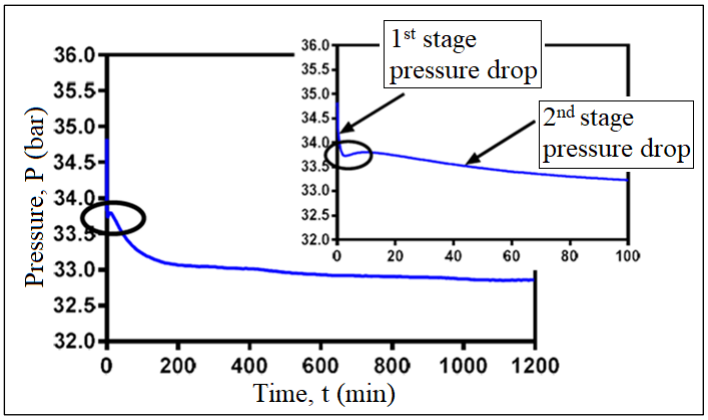

Figure 1. P-t curves that show two-stage pressure drop in 1,200 minutes and the first 100 minutes at the experimental conditions of 35 bar and 275 K

The complete dissolution of CO_2 in water inside silica gel pores was observed after the pressure dropped approximately from 35 bar to 33.8 bar as indicated by point **a–c** (the first stage of pressure drops). Initially, point **a-b** indicates that the dissolution of CO_2 in water happened at around five minutes in which Sloan et al. [33] stated that upon dissolution of gas in water, labile clusters form immediately. Concurrently, labile clusters started to agglomerate by sharing faces, thus increasing disorder, which explained no pressure drop from point **b–c**. This process continued until the size of the cluster agglomerate reached a critical value at point **c** wherein Sloan et al. [33] said this was the point where primary nucleation happens. Also, Tang et al. [28] described the time from point **a–c** as an induction time for hydrate formation. Moreover, the fast induction time observed in this work, which was around 10 minutes, by employing FBR agreed with the one reported in the literature [7-9, 11]. Then, the second stage of pressure drop was observed immediately after point **c** and this significant pressure drop is known as the hydrate growth stage until no more drop-in pressure was observed in batch FBR as indicated by point **d**. Finally, several stages of pressure drop were observed after 100 minutes (point **d**) before it reached a plateau approximately at 1,000 minutes.

CO_2 solubility in water

Since the experiments were conducted in batch mode or isochoric condition, the total number of moles of CO_2 consumed can easily be calculated by using the Ideal Gas law equation. Then, the mole fraction of CO_2 dissolved in water was calculated to be 0.0438 where the value of Henry's constant at 275 K was obtained from Carrol et al. [32]. This value was not considered for the justification of hydrate formation because the value of Henry's constant in their work was calculated at atmospheric pressure that was not the same with the operating pressures employed in this work. However, this value was presented in the figure for the comparison purpose. Thus, the equilibrium mole fraction of CO_2 in water at various operating temperatures and pressures plotted by Servio et al. [29] was used as a guideline to determine the formation of hydrate in the system. The formation of hydrate was confirmed when the

total experimental mole fraction was higher than the equilibrium mole fraction at the experimental conditions (275 K and 35 bar). Based on the data given by Servio et al. [29], the equilibrium mole fraction was found to be 0.0165 at these experimental conditions.

Figure 2(a) illustrates the total mole fraction of CO_2 consumed in water for all samples throughout the experiments, while Figure 2(b) illustrates the mole fraction of CO_2 consumed during hydrate growth. The red-dashed line in Figure 2(a) shows the total CO_2 dissolved in water at the experimental conditions in which further CO_2 consumed after that is known as the growth of hydrate. The total mole fraction of CO_2 involved in hydrate formation was 0.060 as shown in Figure 2(b). Since the formation of hydrate was justified, the study on final water to hydrate conversion, CO_2 uptake, and rate of hydrate formation are presented in the next section.

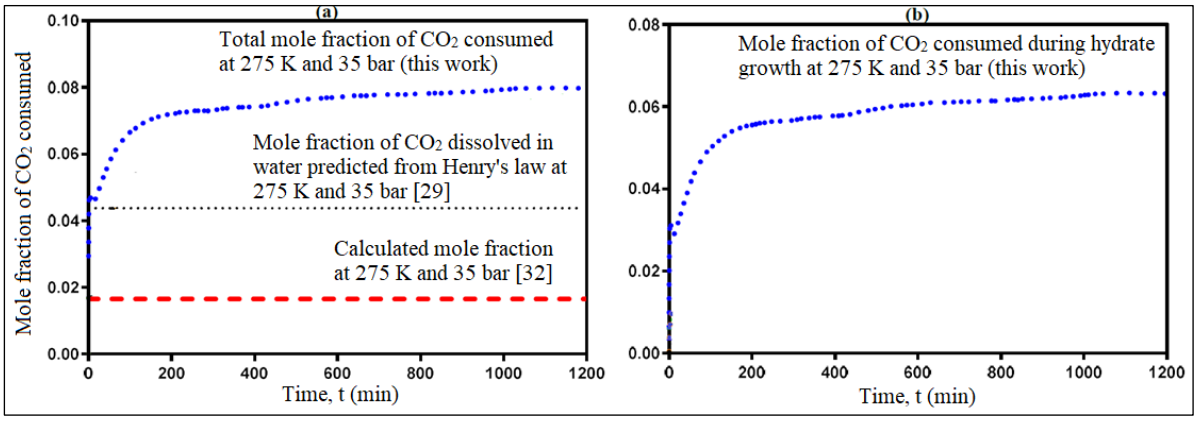

Figure 2. Mole fraction of CO_2 in water inside silica gel pores in 1,200 minutes; (a) total mole fraction of CO_2 and (b) mole fraction of CO_2 during hydrate growth

Control experiments

Six control experiments were performed by using silica contacted with water at various operating conditions. Initially, several experiments using wet (two experiments) and dry (two controlled experiments) silica gels, respectively, were performed to distinguish the formation of hydrate and physical adsorption in the HPVA. Then, the experiments at various operating pressures and temperatures (four controlled experiments; outside hydrate forming region) were performed to further investigate the formation of hydrate in the HPVA.

CO_2 adsorption profile for dry and wet silica gel

Dry silica gel was prepared by using a degassing unit. The sample was dried at 100 ^oC for one night before the commencement of the experiment. The experiments on wet and dry silica gels were performed at the same operating pressure (36 bar) and different operating temperatures (275 K and 298 K, respectively). Figure 3 illustrates the P-t curves for wet and dry silica gels in 600 minutes. The rapid one-stage pressure drops obtained for dry silica gel at both operating temperatures was expected due to normal physical adsorption. The experiment conducted at 298 K on wet silica gel gave slight one-stage pressure drop and was expected due to the normal solubility of CO_2 in water. Further investigation of mole fraction of CO_2 dissolved in water at this operating temperature is presented in the next section. Two-stage pressure drop was observed for the experiment using wet silica gel executed at 275 K due to the formation of hydrate as previously explained. The nucleation stage started after almost 10 minutes and this is known as the induction time for CO_2 hydrate formation. Next, the hydrate growth stage was seen in which the pressure drops of 1 bar occurred after almost 550 minutes. Then, the constant pressure until 600 minutes indicated the end of hydrate formation. Thus, the formation of hydrate in the HPVA was confirmed.

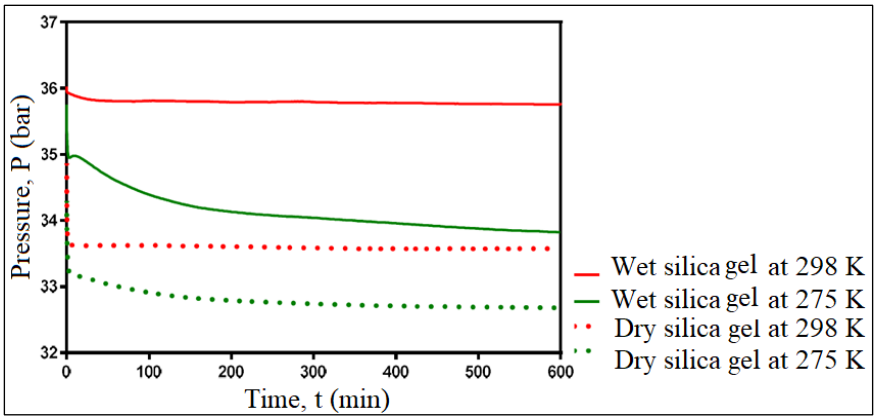

Figure 3. P-t curves for dry and wet silica gels at the operating pressure of 36 bar and temperatures of 275 K and 298 K in 600 minutes

Various operating conditions

More hydrate formation experiments were investigated within and outside of hydrate forming conditions. Table 1 summarizes the operating conditions together with their calculated driving force (ΔP) in which the equilibrium pressure at each operating temperature was obtained from the experimental data plotted by Yang et al. [22].

Table 1. Experimental operating conditions with their respective calculated driving force

Exp.	Operating temperature (K)	Operating pressure (bar)	Equilibrium pressure (bar)	Driving force, ΔP (bar)	Hydrate forming region
1	275	36	17	19	Yes
2	275	30	17	13	Yes
3	275	22	17	5	Yes
4	280	36	30	6	Yes
5	280	26	30	-	No
6	288	36	-	-	No
7	293	36	-	-	No
8	298	36	-	-	No

The study on CO_2 solubility in water at these various operating conditions was performed to justify the formation of hydrate. However, only one P-t curve (experimental conditions of 22 bar and 275 K) was presented, as illustrated in Figure 4 due to the same trend (either two or several stages of pressure drop) observed for all experiments that exhibited hydrate formation. Then, further study on CO_2 uptake was executed for the experiments that exhibited hydrate formation.

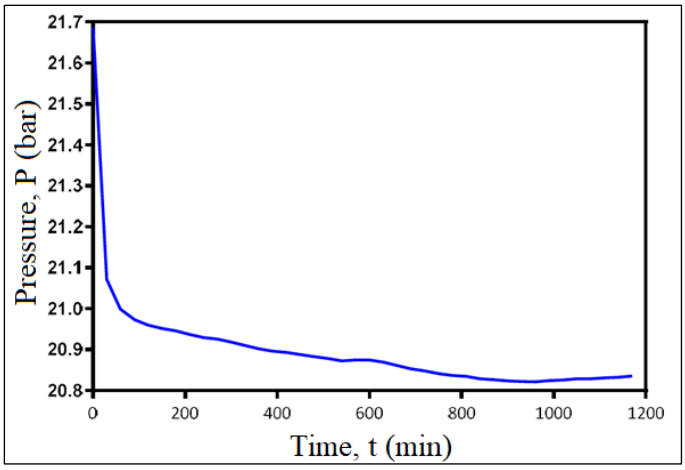

Figure 4. P-t curves that show several stages of pressure drop in 1200 minutes at the experimental conditions of 22 bar and 275 K

CO_2 solubility in water

The analysis of solubility of CO_2 in water was done according to Servio et al. [29] for experiments executed within hydrate forming conditions and Diamond et al. [34] for experiments performed outside hydrate forming regions. Based on the data plotted by Servio et al. [29], the solubility of CO_2 in water in the presence of hydrate at 36 bars was 0.0165 mole fraction of CO_2 at 275 K and 0.021 mole fraction of CO_2 at 280 K. The plotted data also showed that at 275 K, the solubility of CO_2 was the same at pressure ranges from 20 bar to 60 bar. Thus, the value of 0.0165 was also chosen for the operating pressure of 22 bar and 30 bar, at the operating temperature of 275 K. According to data plotted by Diamond et al. [34], the solubility of CO_2 in water at 280 K and 26 bars was 0.023 mole fraction of CO_2. The value observed at 36 bars was 0.022 mole fraction of CO_2 at 288 K, 0.021 mole fraction of CO_2 at 293 K, and 0.018 mol fraction of CO_2 at 298 K. Figures 5 & 6 illustrate the mole fraction of CO_2 dissolved in water at hydrate forming conditions in 600 minutes.

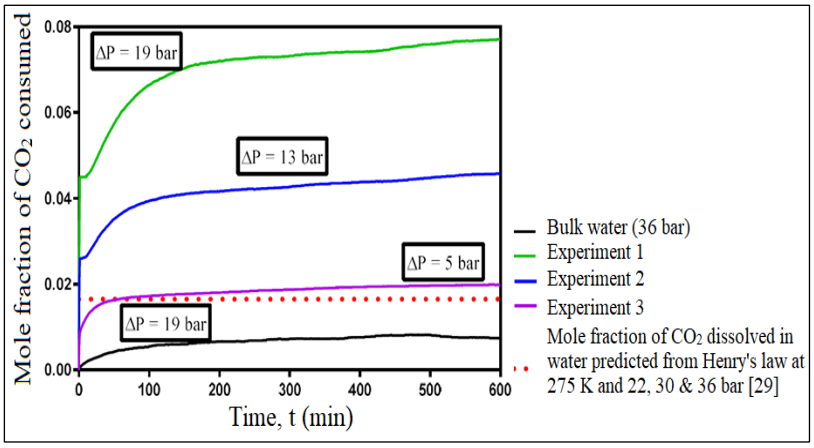

Figure 5. Mole fraction of CO_2 consumed at the operating temperature of 275 K and various driving forces (ΔP) in 600 minutes

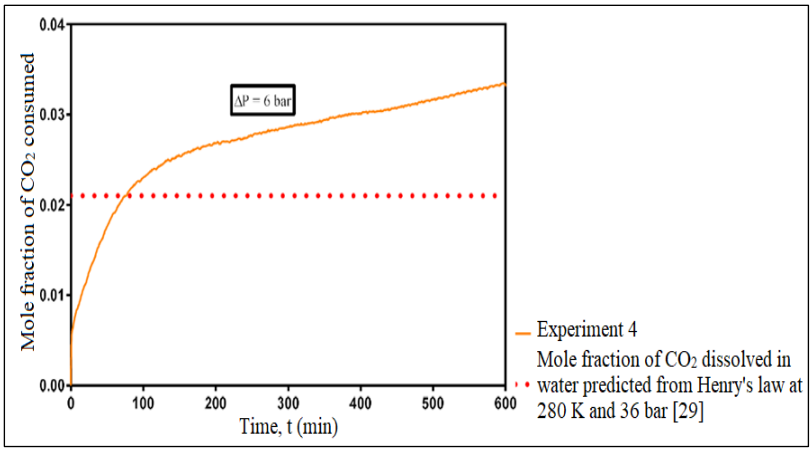

Figure 6. Mole fraction of CO_2 consumed at the operating conditions of 280 K and 36 bars in 600 minutes

It was observed that the total mole fraction of CO_2 soluble in water for Experiments 1 (275 K and 36 bar), 2 (275 K and 30 bar), 3 (275 K and 22 bar), and 4 (280 K and 36 bar) was higher than the value recorded by Servio et al. [29]. The CO_2 consumption obtained before it reached the red-dashed line was assumed to have been caused by the formation of labile clusters. Hence, further CO_2 consumption observed after that was due to the formation of CO_2 hydrate. The total mole fraction of CO_2 dissolved in water increased drastically as the driving force increased, which also justified the formation of CO_2 hydrate. The highest value observed was from Experiment 1 with the driving force of 19 bar, followed by Experiment 2 (driving force of 13 bar), Experiment 4 (driving force of 6 bar), and Experiment 3 (driving force of 5 bar). Even though the driving force for Experiments 3 and 4 was almost the same, only minimal hydrate growth was observed for Experiment 3 due to the low pressure in the system. This indicates that in hydrate forming regions, hydrate formation is easily enhanced by increasing the pressure rather than lowering the temperature. In contrast, the experiment by employing bulk water did not show any hydrate formation at all after 600 minutes, as shown in Figure 6, which explained the importance of a porous medium replacing the stirring process in bulk water system.

Figure 7 illustrates the mole fraction of CO_2 dissolved in water at non-hydrate forming conditions in 600 minutes. It was observed that the total mole fraction of CO_2 soluble in water for Experiments 5 (280 K and 26 bar), 7 (293 K and 36 bar), and 8 (298 K and 36 bar) was lower than the equilibrium mole fraction of CO_2 in water presented by Diamond et al. [34]. However, a small amount of CO_2 dissolved in water was observed which was higher than the equilibrium mole fraction of CO_2 for Experiment 6 (288 K and 36 bar). In summary, in the hydrate forming region, the equilibrium mole fraction of CO_2 in water was reduced as the temperature decreased [29]. Thus, the highest solubility of CO_2 observed in water at the lowest temperature in this study was due to the existence of CO_2 hydrate. In contrast, the solubility of CO_2 in water reduced as the temperature increased in the non-hydrate forming region. This trend was comparable to the equilibrium mole fraction of CO_2 in water as shown in the literature [34], which explains the non-existence of hydrate at these conditions.

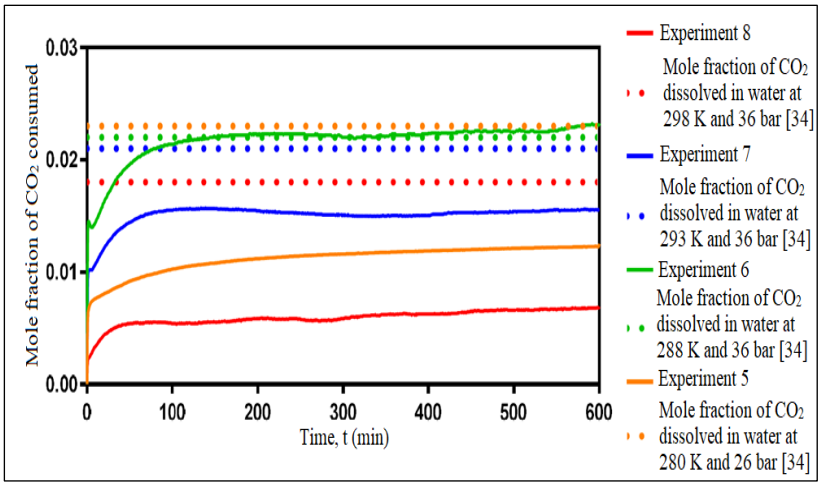

Figure 7. Mole fraction of CO_2 consumed at the non-hydrate forming conditions (Experiments 5– 8) in 600 minutes

High driving force enhanced water conversion to hydrate and gas uptake

The study on CO_2 uptake was performed for Experiments 1–4 where CO2 hydrate was previously found to exist at these experimental operating conditions. The average weight of wet silica gel used was 0.5 g, which led to a total of 0.004 moles of water. All experiments were analysed for a 600-minute period as this was the average time for the hydrate formation to be completed. Table 2 shows that Experiment 1 had the highest CO_2 uptake with a value of 3.75 ± 0.01mmol of CO_2 per g of H_2O, followed by Experiment 2 (1.65 ± 0.18mmol of CO_2 per g of H_2O), Experiment 4 (0.56 ± 0.03mmol of CO_2 per g of H_2O), and finally Experiment 3 (0.26 ± 0.02mmol of CO_2 per g of H_2O). All experiments had relatively low CI, which showed good reproducibility of the experiments at these various operating conditions.

Table 2. Summary of results for hydrate formation experiments perfo**rmed at various hydrate forming** conditions in 600 minutes (Experiments 1–4)

Exp.	Operating conditions	Driving force, ΔP (bar)	Replication	CO_2 uptake (mmol of CO_2/g of H_2O)	Mean CO_2 uptake (mmol of CO_2/g of H_2O)
1	275 K & 36 bars	19	1 2	3.74 3.75	3.75±0.01
2	275 K & 30 bars	13	1 2	1.77 1.52	1.65±0.21
3	275 K & 22 bars	5	1 2	0.23 0.27	0.26±0.02
4	280 K & 36 bars	6	1 2	0.54 0.58	0.56±0.03

The conversion of water to hydrate and gas uptake for Experiments 1–4 with their respective error bars are presented in Figure 8. The highest driving force experiment (Experiment 1 with the driving force of 19 bar) converted the highest water to hydrate with 40 mol% in 600 minutes, which was 50% higher than Experiment 2. This was followed by Experiment 2, almost 16 mol% higher than Experiment 3. These three experiments were executed at 275 K with Experiment 3 having the lowest driving force (5 bar). Furthermore, Experiment 4, which

was performed at higher temperature (280 K) but with ΔP of 6 bar, exhibited 50% greater result as compared to Experiment 3. This indicated that the increased driving force enhanced the formation of CO_2 hydrate.

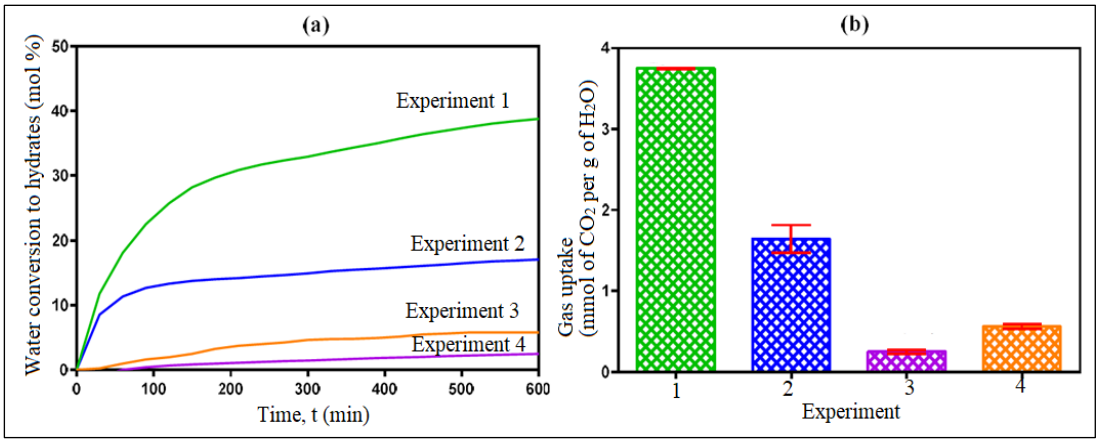

Figure 8. Comparison of (a) water conversion to hydrate and (b) CO_2 uptake at the hydrate forming conditions in 600 minutes

Conclusion

The solubility of CO_2 in water using Henry's law and the experimental pressure–time (P-t) curve were analysed to determine the formation of hydrate. Hydrate formation was confirmed when the mole fraction of CO_2 dissolved in water exceeded the Henry's law value as well as a two-stage pressure drop in the experimental P-t curve. Several experiments that were investigated in the HPVA at various operating conditions justified that hydrate formation only occurred at hydrate forming conditions with the lowest CO_2 uptake of 0.26±0.02 mmol of CO_2 per g of H_2O at 22 bars and 275 K and the highest CO_2 uptake of 3.75±0.01 mmol of CO_2 per g of H_2O at 36 bars and 275 K. In the hydrate forming region, the equilibrium mole fraction of CO_2 in water was reduced as the temperature decreased. Thus, the highest solubility of CO_2 observed in water at the lowest temperature in this study was due to the existence of CO_2 hydrate. In contrast, the solubility of CO_2 in water reduced as the temperature increased in the non-hydrate forming region, which explains the non-existence of hydrate.

Acknowledgement

The authors gratefully acknowledge the Ministry of Higher Education and Islamic Science University of Malaysia (USIM) for their financial support in this work (Grant number: PPPI/FST/0217/051000/12118).

References

1. Caitlyn, K. (2014). Climate change: Atmospheric carbon dioxide. https://www.climate.gov/news-features/understanding-climate/climate-change-atmospheric-carbon-dioxide. [Access online 20 January 2015].
2. Biello, D. (2013). 400 ppm: Carbon dioxide in the atmosphere reaches prehistoric levels. http://blogs.scientificamerican.com/observations/2013/05/09. [Access online 20 January 2015].
3. Kunze, C. and Spliethoff, H. (2012). Assessment of oxy-fuel, pre- and post-combustion-based carbon capture for future IGCC plants. *Applied Energy*, 94: 109-116.
4. IEA (2008). Energy technology perspectives. OECD/IEA Publications 9, Paris: pp. 55-57.
5. Metz, B., Davidson, O., Coninck, H. D., Loos, M. and Meyer, L. (2005). IPCC special report on carbon dioxide capture and storage. Intergovernmental Panel on Climate Change, New York pp. 109-110.
6. D'Alessandro, D. M., Smit, B and Long, J. R. (2010). Carbon dioxide capture: Prospects for new materials. *Angewandte Chemie International Edition*, 49: 6058-6082.
7. Zheng, J., Lee, Y. K., Babu, P., Zhang, P. and Linga, P. (2016). Impact of fixed bed reactor orientation, liquid saturation, bed volume and temperature on the clathrate hydrate process for pre-combustion capture. *Journal of Natural Gas Science and Engineering*, 35:1499-1510.

8. Babu, P., Ho, C.Y., Kumar, R. and Linga, P. (2014). Enhanced kinetics for the clathrate process in a fixed bed reactor in the presence of liquid promoters for pre-combustion carbon dioxide capture. *Energy*, 70: 664-673.
9. Linga, P., Kumar, R. and Englezos, P. (2007). Gas hydrate formation from hydrogen/carbon dioxide and nitrogen/carbon dioxide gas mixtures. *Chemical Engineering Science*, 62: 4268-4276.
10. McCallum, S. D., Riestenberg, D. E., Zatsepina, O. Y. and Phelps, T. J. (2005). Effect of pressure vessel size on the formation of gas hydrates. *Journal of Petroleum Science & Engineering*, 56: 54-64.
11. IEA Clean Coal Centre (2011). Pre-combustion capture of CO_2 in IGCC plants No 11/14, London: pp.11-14.
12. Babu, P., Kumar, R. and Linga, P. (2013). Pre-combustion capture of CO_2 in a fixed bed reactor using the Clathrate hydrate process. *Energy*, 50: 364-373.
13. Carroll, J. (2009). Natural gas hydrates (a guide for engineers). Elsevier Inc., Burlington: pp. 1-15.
14. Adeyemo, A., Kumar, R., Linga, P., Ripmeester., J. and Englezos, P. (2010). Capture of CO_2 from flue or fuel gas mixtures by clathrate crystallization in a silica gel column. *International Journal of Greenhouse Gas Control*, 4: 478-485.
15. Kumar, A., Sakpal, T., Linga, P. and Kumar, R. (2013). Influence of contact medium and surfactants on carbon dioxide Clathrate hydrate kinetics. *Fuel*, 105: 664-671.
16. Park, S., Lee, S., Lee, Y., Lee, Y. and Seo, Y. (2013). Hydrate-based pre-combustion capture of carbon dioxide in the presence of a thermodynamic promoter and porous silica gels. *International Journal of Greenhouse Gas Control*, 14: 193-199.
17. Kang, S. P., Lee, J. and Seo, Y. (2013). Pre-combustion capture of CO_2 by gas hydrate formation in silica gel pore structure. *Chemical Engineering Journal*, 218: 126-132.
18. Mekala, P., Busch, M., Mech, D. and Patel, R. S. (2014). Effect of silica sand size on the formation kinetics of CO_2 hydrate in porous media in the presence of pure water and seawater relevant for CO_2 sequestration. *Journal of Petroleum Science & Engineering*, 122: 1-9.
19. Xiaoya, Z., Jianwei, D.U., Deqing, L., Shuanshi, F. and Cuiping, T. (2009). Influence of A-type zeolite on methane hydrate formation. *Chinese Journal of Chemical Engineering*, 17: 854-859.
20. Zhong, D. L., Li, Z., Lu, Y. Y., Wang, J. L., Yan, J. and Qing, S. L. (2016). Investigation of CO_2 capture from a CO_2 + CH_4 gas mixture by gas hydrate formation in the fixed bed of a molecular sieve. *Industrial & Engineering Chemistry Research*, 55(29): 7973-7980.
21. Mohd Hafiz, A. H., Snape, C. E. and Stevens, L. (2018). Bed height of zeolite affected CO_2 hydrate formation using high pressure volumetric analyser. *Asian Journal of Chemistry*, 30(10): 2269-2272.
22. Yang, M., Song, Y., Liu, W., Zhao, J., Ruan, X., Jiang, L. and Li, Q. (2013). Effects of additive mixtures (THF/SDS) on carbon dioxide hydrate formation and dissociation in porous media. *Chemical Engineering Science*, 90: 69-76.
23. Mohd Hafiz, A.H., Snape, C.E. and Stevens, L. (2018b). The effect of silica particle sizes and promoters to equilibrium moisture content for CO_2 hydrate formation in HPVA. *AIP Conference Proceedings*, 1972: 030019.
24. Babu, P., Linga, P., Kumar, R. and Englezos, P., (2015). A review of the hydrate-based gas separation (HBGS) process for carbon dioxide pre-combustion capture. *Energy*, 85: 261-279.
25. Babu, P., Kumar, R. and Linga, P. (2013b). A new porous material to enhance the kinetics of clathrate process: Application to precombustion carbon dioxide capture. *Environmental Science Technology*, 47: 13191-13198.
26. Skarstrom, C. W. (1960). Method and apparatus for fractionating gaseous mixtures by adsorption. US Patent, No: 2944627.
27. Grande, C. A. (2012). Advances in pressure swing adsorption for gas separation. *ISRN Chemical Engineering Science*, 2012: 1-13.
28. Tang, J., Zeng, D., Wang, C., Chen, Y., He, L. and Cai, N. (2013). Study on the influence of SDS and THF on hydrate-based gas separation performance. *Chemical Engineering Research and Design*, 91: 1777-1782.
29. Servio, P. and Englezos, P. (2001). Effect of temperature and pressure on the solubility of carbon dioxide in water in the presence of gas hydrate. *Fluid Phase Equilibria*, 190: 127-134.
30. Dawson, R., Stevens, L. A., Williams, O. S. A., Wang, W., Carter, B. O., Sutton, S., Drage, T. C., Blanc, F., Adams, D. J. and Cooper, A. I. (2014). Dry bases: carbon dioxide capture using alkaline dry water. *Energy & Environmental Science*, 7: 1786-1791.

31. Mohd Hafiz, A. H., Snape, C. E. and Stevens, L. (2017). Enhance CO_2 hydrate formation inside the HPVA by vigorous stirring during sample preparation. *Proceeding of Postgraduate Seminar on Science and Technology*, 7th November 2016, Nilai, Malaysia.
32. Carrol, J., Slupsky, J. and Mather, E. (1991). The solubility of CO_2 in water at low pressure. *Journal of Physic and Chemistry*, 20: 1201-1209.
33. Sloan, E. D. and Koh, C. A. (2008). Clathrate hydrates of natural gases. Taylor & Francis Group, Boca Raton: pp. 130-138.
34. Diamond, L. W. and Akinfiev, N. N. (2003). Solubility of CO_2 in water from -1.5 to 100 ^oC and from 0.1 to 100 MPa: Evaluation of literature data and thermodynamic modelling. *Fluid Phase Equilibria*, 208: 265-290.
35. Babu, P., Ong, H. W. N. and Linga, P. (2016). A systematic kinetic study to evaluate the effect of tetrahydrofuran on the clathrate process for pre-combustion capture of carbon dioxide. *Energy*, 94: 431-442.